Article

Solvent Effects on the Oxidation of RuO to ORuO by MnO. Hydrogen-Atom versus Oxygen-Atom Transfer

William W. Y. Lam, Wai-Lun Man, Chi-Fai Leung, Chun-Yuen Wong, and Tai-Chu Lau

J. Am. Chem. Soc., **2007**, 129 (44), 13646-13652• DOI: 10.1021/ja074282f • Publication Date (Web): 12 October 2007

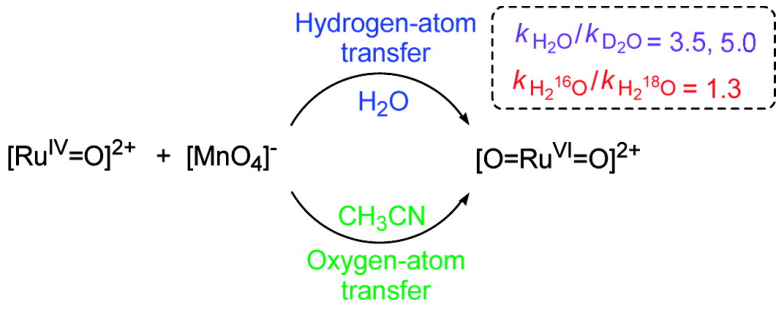

More About This Article

Additional resources and features associated with this article are available within the HTML version:

- Supporting Information
- Links to the 1 articles that cite this article, as of the time of this article download
- Access to high resolution figures
- Links to articles and content related to this article
- Copyright permission to reproduce figures and/or text from this article

View the Full Text HTML

J|A|C|S
ARTICLES
Published on Web 10/12/2007

Solvent Effects on the Oxidation of Ru^{IV}=O to O=Ru^{VI}=O by MnO_4^-. Hydrogen-Atom versus Oxygen-Atom Transfer

William W. Y. Lam, Wai-Lun Man, Chi-Fai Leung, Chun-Yuen Wong, and Tai-Chu Lau*

Contribution from the Department of Biology and Chemistry, City University of Hong Kong, Kowloon Tong, Hong Kong

Received June 13, 2007; E-mail: bhtclau@cityu.edu.hk

Abstract: The kinetics of the oxidation of *trans*-[Ru^{IV}(tmc)(O)(solv)]$^{2+}$ to *trans*-[Ru^{VI}(tmc)$(O)_2$]$^{2+}$ (tmc is 1,4,8,-11-tetramethyl-1,4,8,11-tetraazacyclotetradecane, a tetradentate macrocyclic tertiary amine ligand; solv = H_2O or CH_3CN) by MnO_4^- have been studied in aqueous solutions and in acetonitrile. In aqueous solutions the rate law is $-d[MnO_4]/dt = k_{H_2O}[Ru^{IV}][MnO_4^-] = (k_x + (k_y)/(K_a)[H^+])[Ru^{IV}][MnO_4^-]$, $k_x = (1.49 \pm 0.09) \times 10^1$ M^{-1} s^{-1} and $k_y = (5.72 \pm 0.29) \times 10^4$ M^{-1} s^{-1} at 298.0 K and $I = 0.1$ M. The terms k_x and k_y are proposed to be the rate constants for the oxidation of Ru^{IV} by MnO_4^- and $HMnO_4$, respectively, and K_a is the acid dissociation constant of $HMnO_4$. At $[H^+] = I = 0.1$ M, $\Delta H^{\ddagger}$ and $\Delta S^{\ddagger}$ are (9.6 ± 0.6) kcal mol^{-1} and $-(18 \pm 2)$ cal mol^{-1} K^{-1}, respectively. The reaction is much slower in D_2O, and the deuterium isotope effects are $k_x/k_x^D = 3.5 \pm 0.1$ and $k_y/k_y^D = 5.0 \pm 0.3$. The reaction is also noticeably slower in $H_2{}^{18}O$, and the oxygen isotope effect is $k_{H_2}{}^{16}{}_O/k_{H_2}{}^{18}{}_O = 1.30 \pm 0.07$. ^{18}O-labeled studies indicate that the oxygen atom gained by Ru^{IV} comes from water and not from $KMnO_4$. These results are consistent with a mechanism that involves initial rate-limiting hydrogen-atom abstraction by MnO_4^- from coordinated water on Ru^{IV}. In acetonitrile the rate law is $-d[MnO_4^-]/dt = k_{CH_3CN}[Ru^{IV}][MnO_4^-]$, $k_{CH_3CN} = 1.95 \pm 0.08$ M^{-1} s^{-1} at 298.0 K and $I = 0.1$ M. $\Delta H^{\ddagger}$ and $\Delta S^{\ddagger}$ are (12.0 ± 0.3) kcal mol^{-1} and $-(17 \pm 1)$ cal mol^{-1} K^{-1}, respectively. ^{18}O-labeled studies show that in this case the oxygen atom gained by Ru^{IV} comes from MnO_4^-, consistent with an oxygen-atom transfer mechanism.

1. Introduction

High-valent metal-oxo species are active intermediates in a variety of enzymatic and catalytic oxidation processes.[1,2] Metal-oxo species are usually prepared by oxygen-atom transfer[3] from an oxygen donor XO to a metal precursor.

$$(L)M^n + XO \rightarrow (L)M^{(n+2)}{=}O + X \qquad (1)$$

They can also be formed via loss of electrons and protons from an aqua species, using either chemical or electrochemical methods.[4]

$$(L)M^n - OH_2 \rightarrow (L)M^{(n+1)} - OH + H^+ + e^- \qquad (2)$$

$$(L)M^{(n+1)} - OH \rightarrow (L)M^{(n+2)}{=}O + H^+ + e^- \qquad (3)$$

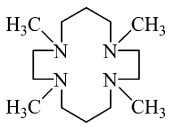

Figure 1. Structure of tmc.

The loss of an electron and a proton can proceed by stepwise pathways involving initial electron transfer or initial proton transfer or by a concerted pathway involving hydrogen-atom transfer.[5]

We report here a study of the oxidation of a ruthenium(IV) oxo species containing a macrocyclic tertiary amine ligand, *trans*-[Ru^{IV}(tmc)(O)(solv)]$^{2+}$ (tmc = 1,4,8,11-tetramethyl-1,4,8,-11-tetraazacyclotetradecane, Figure 1; solv = H_2O or CH_3CN) by MnO_4^- in water and in acetonitrile. In both solvents the

(1) *Biomimetic Oxidations Catalyzed by Transition Metal Complexes*; Meunier, B., Ed.; Imperial College Press: London, 2000.
(2) *Metal-Oxo and Metal-Peroxo Species in Catalytic Oxidations*; Meunier, B., Ed.; Springer-Verlag: Berlin, 2000.
(3) (a) Holm, R. H. *Chem. Rev.* **1987**, *87*, 1401−1449. (b) Woo, L. K. *Chem. Rev.* **1993**, *93*, 1125−1136.
(4) See for example: (a) Meyer, T. J.; Huynh, M. H. V. *Inorg. Chem.* **2003**, *42*, 8140−8160. (b) Moyer, B. A.; Meyer, T. J. *Inorg. Chem.* **1981**, *20*, 436−444. (c) Binstead, R. A.; Moyer, B. A.; Samuls, G. J.; Meyer, T. J. *J. Am. Chem. Soc.* **1981**, *103*, 2897−2899. (d) Moyer, B. A.; Meyer, T. J. *J. Am. Chem. Soc.* **1978**, *100*, 3601−3603. (e) Che, C. M.; Yu, W. Y. *Pure Appl. Chem.* **1999**, *71*, 281−288. (f) Che, C. M.; Yam, V. W. W. *Adv. Transition Metal Coord. Chem.* **1996**, *1*, 209−237. (g) Cheng, W. C.; Yu, W. Y.; Cheung, K. K.; Che, C. M. *J. Chem. Soc., Dalton Trans.* **1994**, 57−62. (h) Che, C. M.; Wong, K. Y.; Leung, W. H.; Poon, C. K. *Inorg. Chem.* **1986**, *25*, 345−348.
(5) Hydrogen-atom transfer (HAT) is defined by Mayer as the concerted movement of a proton and an electron in a single kinetic step where both the proton and the electron originate from the same reactant and travel to the same product. HAT is one type of the broad class of proton-coupled electron-transfer (PCET) reactions, which also includes reactions where the proton and electron are separated. (a) Mayer, J. M. *Annu. Rev. Phys. Chem.* **2004**, *55*, 363−390. (b) Mayer, J. M.; Rhile, I. J. *Biochim. Biophys. Acta* **2004**, *1655*, 51−58. (c) Mayer, J. M.; Rhile, I. J.; Larsen, F. B.; Mader, E. A.; Markle, T. F.; DiPasquale, A. G. *Photosynth. Res.* **2006**, *87*, 3−20. (d) Mayer, J. M.; Rhile, I. J.; Larsen, F. B.; Mader, E. A.; Markle, T. F.; DiPasquale, A. G. *Photosynth. Res.* **2006**, *87*, 21−24. (e) Mayer, J. M.; Mader, E. A.; Roth, J. P.; Bryant, J. R.; Matsuo, T.; Dehestani, A.; Bales, B. C.; Watson, E. J.; Osako. T.; Valliant-Saunders, K.; Lam, W.-H.; Hrovat, D. A.; Borden, W. T.; Davidson, E. R. *J. Mol. Catal. A: Chem.* **2006**, *251*, 24−33. (f) Mader, E. A.; Davidson, E. R.; Mayer, J. M. *J. Am. Chem. Soc.* **2007**, *129*, 5153−5166.

10.1021/ja074282f CCC: $37.00

Scheme 1

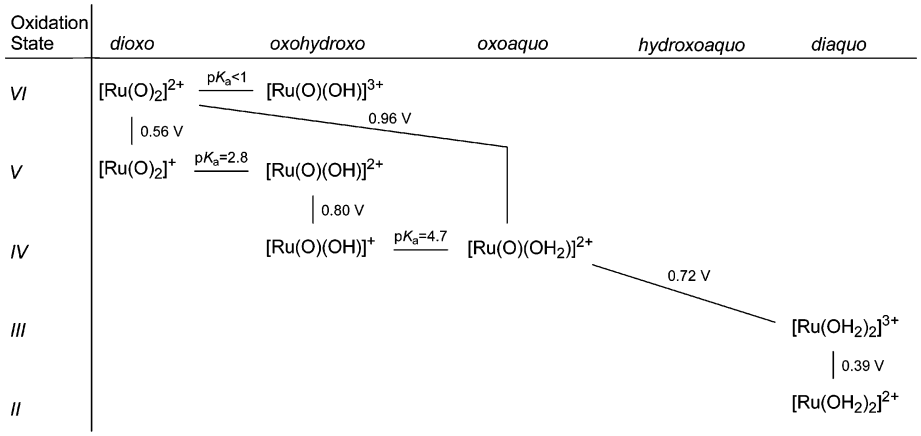

reaction results in a net gain of an oxygen atom by *trans*-[Ru^{IV}(tmc)(O)(solv)]$^{2+}$ to give *trans*-[Ru^{VI}(tmc)$(O)_2$]$^{2+}$ (with loss of solvent). However, we provide evidence herein that the initial rate-limiting step in water occurs by hydrogen-atom transfer, while that in acetonitrile occurs by oxygen-atom transfer.

Thermodynamic data (E^0 vs NHE and pK_a values, 298 K) for the *trans*-[Ru^{VI}(tmc)$(O)_2$]$^{2+}$ system in aqueous solutions are summarized in Scheme 1.[6]

2. Experimental Section

Materials. *trans*-[Ru^{IV}(tmc)(O)$(NCCH_3)$]X_2 (X = ClO_4 or PF_6) was prepared according to a literature method.[7] All chemicals were of reagent grade. Potassium permanganate (Aldrich, 97%) was recrystallized from water.[8] Water for kinetic measurements was distilled twice from alkaline permanganate. D_2O (99.9 atom % D) was obtained from Aldrich. $H_2{}^{18}O$ (97 atom % ^{18}O) was obtained from Medical Isotopes, Inc. Ionic strength and pH were maintained with sodium trifluoroacetate and trifluoroacetic acid, respectively. The pD values for D_2O solutions were determined by using a pH meter (Delta 320) using pD = pH_{meas} + 0.4.

^{18}O-labeled potassium permanganate was prepared according to a literature method.[9] In a typical experiment K[MnO_4] (0.19 g, 1.2 mmol) was refluxed in 97% $H_2{}^{18}O$ (1 g) under argon for 30 h. The dark purple solid was then collected after removal of solvent under vacuum. IR (Nujol mull)/cm^{-1}: $\nu(Mn^{16}O)$, 900; $\nu(Mn^{18}O)$, 868.

Instrumentation. Kinetic experiments were done by using a Hewlett-Packard 8452A diode-array spectrophotometer. IR spectra were recorded as KBr pellets on a Nicolet Avatar 360 FT-IR spectrophotometer at 4 cm^{-1} resolution. Electrospray ionization mass spectra (ESI/MS) were obtained on a PE SCIEX API 365 mass spectrometer. The analyte solution was continuously infused with a syringe pump at a constant flow rate of 5 μL min^{-1} into the pneumatically assisted electrospray probe with nitrogen as the nebulizing gas. The declustering potential was typically set at 10−20 V.

Kinetics. The concentrations of Ru^{IV} were at least in 10-fold excess of that of MnO_4^-. The reaction progress was monitored by observing absorbance changes at 270 or 526 nm. Pseudo-first-order rate constants, k_{obs}, were obtained by nonlinear least-square fits of A_t vs time t according to the equation $A_t = A_\infty + (A_0 - A_\infty)\exp(-k_{obs}t)$, where A_0 and A_∞ are the initial and final absorbances, respectively. The effects of temperature were studied over a 30 °C temperature range, activation parameters were obtained by using the Eyring equation.

Products and Stoichiometry. The ruthenium product from the oxidation of Ru^{IV} by MnO_4^- in aqueous solutions was determined as follows. Ru^{IV} (1×10^{-4} M) and MnO_4^- (4×10^{-5} M) were allowed to react. The resulting solution was loaded onto a Sephadex-SP C-25 cation-exchange resin column. By eluting with 0.2 M $HClO_4$ and examining the UV−vis spectrum of the solution, *trans*-[Ru^{VI}(tmc)$(O)_2$]$^{2+}$ [λ_{max}/nm (ϵ/dm^3 mol^{-1} cm^{-1}): 445 (50), 388 (560), ∼305 (sh) (960), 256 (1.03×10^4) and 225 (1.28×10^4)][5] was found to be produced quantitatively.

The pK_a of $HMnO_4$ was determined by a standard spectrophotometric method.[10] The spectra of $KMnO_4$ at various H_2SO_4 concentrations were measured (Figure S6, Supporting Information). The spectrum at [H_2SO_4] = 16 M was taken as that of 100% $HMnO_4$. The pK_a was obtained by extrapolating the plot of ($\log([HMnO_4]/[MnO_4^-]) - \log[H^+]$) vs [$H_2SO_4$] to zero ionic strength (Figure S7, Supporting Information). The pK_a of $DMnO_4$ was determined similarly by using D_2O.

Warning. Permanganate is a strong oxidizer in strongly acidic solutions. Although we have not encountered any explosions so far, the amount of potassium permanganate used each time should be less than 50 mg.

3. Results and Discussion

3.1. Reaction in Water. 3.1.1. Spectral Changes and Stoichiometry. *trans*-[Ru^{IV}(tmc)(O)(OH_2)]$^{2+}$ was generated in situ by dissolving *trans*-[Ru^{IV}(tmc)(O)$(NCCH_3)$]$^{2+}$ in water. Figure 2 shows the spectral changes upon mixing *trans*-[Ru^{IV}(tmc)(O)(OH_2)]$^{2+}$ (5×10^{-5} M) with MnO_4^- (4×10^{-5} M) in 0.01 M H^+ and I = 0.01 M at 298.0 K. Well-defined isosbestic points at 292, 390, 422, and 604 nm were maintained throughout the reaction. Analysis of the solution after cation-exchange chromatography indicates quantitative formation of *trans*-[Ru^{VI}(tmc)$(O)_2$]$^{2+}$. In a separate experiment a 5.2×10^{-4} M solution of *trans*-[Ru^{IV}(tmc)(O)(OH_2)]$^{2+}$ was mixed with a 5.2×10^{-4} M of MnO_4^- at [H^+] = I = 0.1 M. Analysis of the [MnO_4^-] remaining by monitoring the absorbance at 526 nm indicates that 5 mol of Ru^{IV} reacts with 2 mol of MnO_4^-. Thus the stoichiometry of the reaction can be represented by

$$5[Ru^{IV}(tmc)(O)(OH_2)]^{2+} + 2MnO_4^- + 6H^+ \rightarrow 5[Ru^{VI}(tmc)(O)_2]^{2+} + 2Mn^{2+} + 8H_2O \quad (4)$$

(6) (a) Che, C. M.; Wong, K. Y.; Poon, C. K. *Inorg. Chem.* **1985**, *24*, 1797−1800. (b) Che, C. M.; Lau, K.; Lau, T. C.; Poon, C. K. *J. Am. Chem. Soc.* **1990**, *112*, 5176−5181.
(7) Che, C. M.; Lai, T. F.; Wong, K. Y. *Inorg. Chem.* **1987**, *26*, 2289−2299.
(8) Armarego, W. L. F.; Perrin, D. D. *Purification of Laboratory Chemicals*, 4th ed.; Reed Educational and Professional Publishing Ltd.: Oxford, England, 1996.
(9) Heckner, K.-H. *Z. Phys. Chem.* (Leipzig) **1968**, *239*, 387−394.
(10) Baiely, N.; Carrington, A.; Lott, K. A. K.; Symons, M. C. R. *J. Chem. Soc.* **1960**, 290−297.

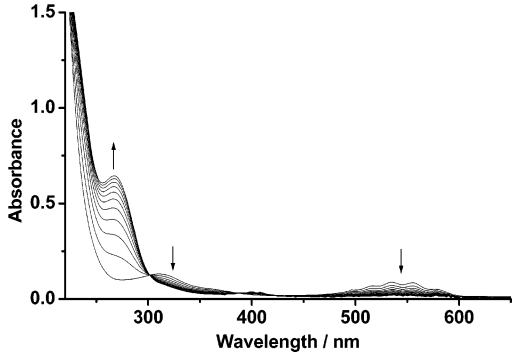

Figure 2. Spectral changes at 200 s intervals for the oxidation of *trans*-$[Ru^{IV}(tmc)(O)(OH_2)]^{2+}$ (5×10^{-5} M) by MnO_4^- (4×10^{-5} M) in 0.01 M H^+ and $I = 0.01$ M at 298.0 K.

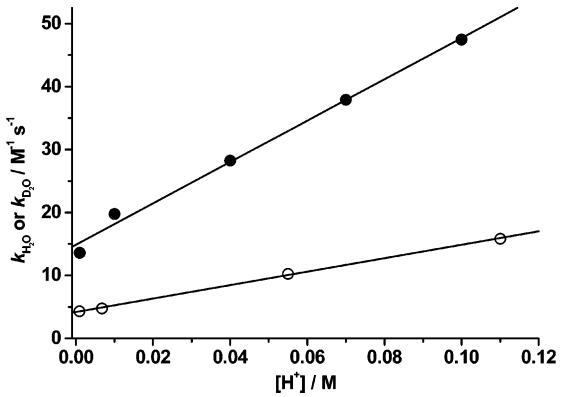

Figure 3. Plot of k_{H_2O} vs $[H^+]$ (solid circle) and $[D^+]$ (open circle) for the oxidation of *trans*-$[Ru^{IV}(tmc)(O)(OH_2)]^{2+}$ by MnO_4^- in aqueous solution at 298.0 K and $I = 0.1$. [For H^+, slope $= (3.29 \pm 0.16) \times 10^2$; *y*-intercept $= (1.49 \pm 0.09) \times 10^1$; $r = 0.997$. For D^+, slope $= (1.06 \pm 0.02) \times 10^2$; *y*-intercept $= (4.18 \pm 0.14)$; $r = 0.999$.]

3.1.2. Kinetics. The kinetics of the reaction were monitored at either 270 or 526 nm. The rate constants obtained are the same at both wavelengths. In the presence of at least 10-fold excess of Ru^{IV}, clean pseudo-first-order kinetics were observed for over three-half-lives. The pseudo-first-order rate constant, k_{obs}, is independent of the concentration of MnO_4^- ($1 \times 10^{-5} - 4 \times 10^{-5}$ M) but depends linearly on $[Ru^{IV}]$ (Figure S1, Supporting Information). Thus, the experimentally determined rate law is as shown:

$$-\frac{d[MnO_4^-]}{dt} = k_{H_2O}[MnO_4^-][Ru^{IV}] \quad (5)$$

k_{H_2O} was found to be $(4.75 \pm 0.02) \times 10^1$ M^{-1} s^{-1} at 298.0 K, $[H^+] = I = 0.1$ M. The effects of temperature were studied from 288.0 to 318.0 K at $[H^+] = I = 0.1$ M. $\Delta H^{\ddagger}$ and $\Delta S^{\ddagger}$ were found to be (9.6 ± 0.6) kcal mol^{-1} and $-(18 \pm 2)$ cal mol^{-1} K^{-1}, respectively (Figure S2, Supporting Information).

The effects of acid on the rate constants were investigated at $[H^+] = 0.001-0.1$ M, 298.0 K and $I = 0.1$ M. The plot of k_{H_2O} versus $[H^+]$ is linear (Figure 3), this is consistent with the reaction scheme shown in eqs 6−8. In acidic medium MnO_4^- is known to be protonated to give $HMnO_4$, which has been isolated and characterized.[11] Similar acid-dependent behavior have also been observed in the oxidation of other species by MnO_4^-.[12−14]

$$HMnO_4 \overset{K_a}{\rightleftharpoons} H^+ + MnO_4^- \quad (6)$$

$$Ru^{IV} + MnO_4^- \xrightarrow{k_x} \text{products} \quad (7)$$

$$Ru^{IV} + HMnO_4 \xrightarrow{k_y} \text{products} \quad (8)$$

The rate law is shown in eq 9:

$$-\frac{d[MnO_4^-]}{dt} = \left(k_x + \frac{k_y}{K_a}[H^+]\right)[Ru^{IV}][MnO_4^-] \quad (9)$$

A pK_a value of $-(2.24 \pm 0.02)$ was used for $HMnO_4$, which was determined by a standard spectrophotometric method;[10] this value is in agreement with a literature value of -2.25.[10] The values of k_x and k_y were found to be $(1.49 \pm 0.09) \times 10^1$ M^{-1} s^{-1} and $(5.72 \pm 0.29) \times 10^4$ M^{-1} s^{-1}, respectively at 298.0 K and $I = 0.1$ M.

The effects of ionic strength were studied from $I = 0.01-0.1$ M at $H^+ = 0.01$ M. The Debye−Hückel plot[15] of log k_{H_2O} versus $2AI^{1/2}/(1 + I^{1/2})$ is linear (Figure S3, Supporting Information) and the observed slope of $-(2.38 \pm 0.31)$ is consistent with the major reaction pathway being a bimolecular reaction between a 2+ and a 1− ion. At pH = 2.0, the predominant pathway should be the reaction of *trans*-$[Ru^{IV}(tmc)(O)(OH_2)]^{2+}$ with MnO_4^-.

Kinetic Isotope Effects. The kinetics were also carried out in D_2O at pD = 1−3 and the plot of k_{D_2O} versus $[D^+]$ is shown in Figure 3. The pK_a value of $DMnO_4$ in D_2O was determined to be $-(2.03 \pm 0.02)$ using a spectrophotometric method,[10] this gives $K_a^H/K_a^D = 1.6$. Using this K_a^D value, k_x^D and k_y^D, the rate constants for the oxidation of Ru^{IV} by MnO_4^- and $DMnO_4$ in D_2O, respectively, were found to be (4.18 ± 0.14) M^{-1} s^{-1} and $(1.14 \pm 0.02) \times 10^4$ M^{-1} s^{-1}, respectively. Hence the deuterium isotope effects are k_x/k_x^D $(MnO_4^-) = 3.5 \pm 0.1$ and $k_y/k_y^D(HMnO_4) = 5.0 \pm 0.3$.

The kinetics were also carried out in $H_2{}^{18}O$ (97 atom % ^{18}O) at 298.0 K, $[H^+] = 0.001$ M and $I = 0.02$ M.[16] Figure 4 shows plots of k_{obs} vs $[Ru^{IV}]$ in $H_2{}^{16}O$ and $H_2{}^{18}O$. The second-order rate constants, $k_{H_2{}^{16}O}$ and $k_{H_2{}^{18}O}$, were found to be $(1.66 \pm 0.07) \times 10^1$ M^{-1} s^{-1} and $(1.28 \pm 0.03) \times 10^1$ M^{-1} s^{-1}, respectively. The kinetic isotope effect $k_{H_2{}^{16}O}/k_{H_2{}^{18}O} = 1.30 \pm 0.07$.

3.2. Reaction in Acetonitrile. The spectral changes for the oxidation of *trans*-$[Ru^{IV}(tmc)(O)(NCCH_3)]^{2+}$ by MnO_4^- in CH_3CN are shown in Figure 5. The final manganese product is colloidal MnO_2, as shown by its characteristic optical spectrum.[17] The ruthenium product is $[Ru^{VI}(tmc)(O)_2]^{2+}$, as shown by ESI/MS (see section 3.3). In a separate experiment, 5.23×10^{-4} M MnO_4^- and 5.23×10^{-4} M Ru^{IV} were allowed to react; analysis of the amount of MnO_4^- consumed by monitoring the

(11) Frigerio, N. A. *J. Am. Chem. Soc*. **1969**, *91*, 6200−6201.
(12) Thomas, L.; Hicks, K. W. *Inorg. Chem*. **1974**, *13*, 749−752.
(13) McAllister, R.; Hicks, K. W.; Hurless, M. A.; Pittenger, S. T.; Gederidge, R. W. *Inorg. Chem*. **1982**, *21*, 4098−4100.
(14) Moore, F. M.; Hicks, K. W. *Inorg. Chem*. **1975**, *14*, 413−416.
(15) Atkins, P. W. *Physical Chemistry*, 5th ed.; Oxford University Press: Oxford, England, 1994.
(16) The Ru^{IV} complex is significantly less soluble in $H_2{}^{18}O$ than in $H_2{}^{16}O$, in some cases 5% of CH_3CN was added to facilitate dissolution. Control experiments show that the presence of 5% CH_3CN does not affect the rate constants. At 25 °C the solubility of the Ru^{IV} complex in $H_2{}^{16}O$, $H_2{}^{18}O$ (distilled), and $D_2{}^{16}O$ (determined using the UV−vis spectrophotometric method) are 1.64×10^{-3} (±3%), 1.23×10^{-3}, and 1.63×10^{-3} M, respectively.
(17) Gardner, K. A.; Kuehnert, L. L.; Mayer, J. M. *Inorg. Chem*. **1997**, *36*, 2069−2078.

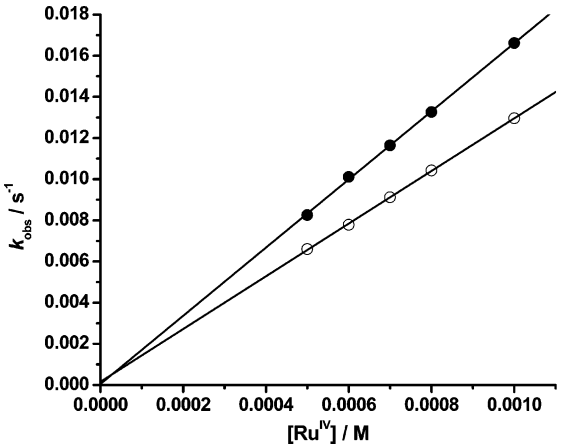

Figure 4. Plots of k_{obs} vs [Ru^{IV}] for the oxidation of *trans*-[Ru^{IV}(tmc)(O)(OH_2)]$^{2+}$ by MnO_4^- (5×10^{-5} M) at 298.0 K, [H^+] = 0.001 M and I = 0.02 M in $H_2{}^{16}O$ (solid circle) and $H_2{}^{18}O$ (open circle). [For $H_2{}^{16}O$, slope = $(1.66 \pm 0.07) \times 10^1$; y-intercept = $(4.93 \pm 45.5) \times 10^{-5}$; r = 0.999. For $H_2{}^{18}O$, slope = $(1.28 \pm 0.03) \times 10^1$; y-intercept = $(1.60 \pm 2.24) \times 10^{-4}$; r = 0.999.]

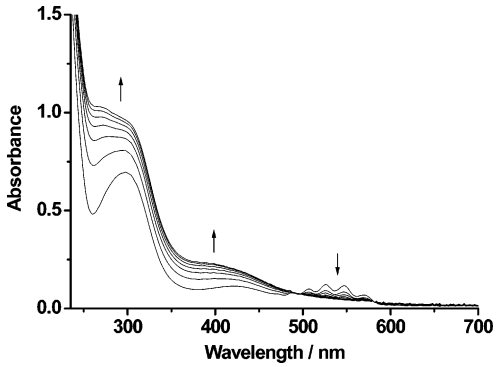

Figure 5. Spectral changes at 420 s intervals for the oxidation of *trans*-[Ru^{IV}(tmc)(O)($NCCH_3$)]$^{2+}$ (5×10^{-4} M) by MnO_4^- (5×10^{-5} M) in CH_3CN at 298.0 K and I = 0.1 M. Isosbestic points are found at 493 and 582 nm.

absorbance at 526 nm indicates that 3 mol of Ru^{IV} reacts with 2 mol of MnO_4^-. Thus the reaction can be represented by

$$3[Ru^{IV}(tmc)(O)(NCCH_3)]^{2+} + 2MnO_4^- + H_2O \rightarrow 3[Ru^{VI}(tmc)(O)_2]^{2+} + 2MnO_2 + 3CH_3CN + 2OH^- \quad (10)$$

The reaction progress was monitored by observing absorbance changes at 526 nm under pseudo-first-order conditions with Ru^{IV} in excess, and the following rate law was obtained

$$-\frac{d[MnO_4^-]}{dt} = k_{CH_3CN}[MnO_4^-][Ru^{IV}] \quad (11)$$

At 298.0 K and I = 0.1 M (maintained with $^nBu_4NPF_6$), the second-order rate constant, k_{CH_3CN}, was found to be 1.95 ± 0.08 M^{-1} s^{-1} (Figure S4, Supporting Information). The effects of temperature were studied from 288.0 to 318.0 K. $\Delta H^{\ddagger}$ and $\Delta S^{\ddagger}$ were found to be (12.0 ± 0.3) kcal mol^{-1} and $-(17 \pm 1)$ cal mol^{-1} K^{-1}, respectively (Figure S5, Supporting Information).

Protons are consumed according to eq 10, presumably they come from trace water in acetonitrile. A few experiments were done with acetic acid added to the solution. At [Ru^{IV}] = 5×10^{-4} M and [MnO_4^-] = 5×10^{-5} M, the pseudo-first-order rate constants at 298.0 K with 0, 2.0×10^{-4}, 2.0×10^{-3}, and 2.0×10^{-2} M of acetic acid present were found to be 9.60×10^{-4}, 1.44×10^{-3}, 1.98×10^{-3}, and 1.95×10^{-3} s^{-1}, respectively, indicating that there is a slight rate acceleration effect of acetic acid.

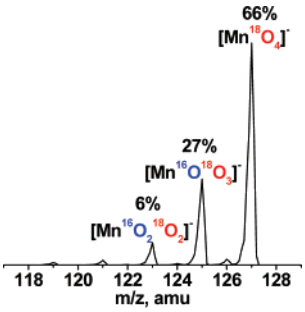

Figure 6. ESI/MS (−ve mode) of ^{18}O-labeled potassium permanganate in acetonitrile.

3.3. ^{18}O-Labeled Study. ^{18}O-labeled permanganate was prepared by refluxing $KMnO_4$ in $H_2{}^{18}O$ (97 atom % ^{18}O). The IR spectrum of the compound shows ν(Mn = ^{18}O) at 868 cm^{-1}, in agreement with the value of 860 cm^{-1} calculated from a simple diatomic harmonic oscillator model using ν(Mn^{16}O) = 900 cm^{-1}. The ESI/MS spectrum of the ^{18}O-labeled compound in CH_3CN (−ve mode) shows peaks at m/z = 121 [Mn(^{16}O)$_3$(^{18}O)]$^-$ (<1% intensity), 123 [Mn(^{16}O)$_2$(^{18}O)$_2$]$^-$ (6%), 125 [Mn(^{16}O)(^{18}O)$_3$]$^-$ (27%), and 127 [Mn(^{18}O)$_4$]$^-$ (66%), with an overall 90 atom % of ^{18}O. (Figure 6). The mass spectrum remains unchanged in $H_2{}^{16}O$ at pH 7 for at least 24 h at 23 °C; however at pH = 3, the ^{18}O-labeled permanganate (3.9×10^{-3} M) exchanges with $H_2{}^{16}O$ with a half-life of ca. 3 h.

3.3.1. Reaction in Water. The ESI/MS (+ve mode) of [Ru^{IV}(tmc)(^{16}O)($NCCH_3$)](PF_6)$_2$ in 1 mM CF_3COOH in $H_2{}^{16}O$ exhibits a peak at m/z = 187.4 which arises from the doubly charged species [Ru^{IV}(tmc)(^{16}O)]$^{2+}$ (Figure 7).[18] Upon adding excess K[$Mn^{18}O_4$] (90% ^{18}O-labeled) this peak gradually decreases with concomitant increase of a new peak at m/z 195.4. Analysis of the peak at m/z = 195.4 at different time intervals (5 min, 30 min, and 1 h) indicates that it is 100% [Ru(tmc)(^{16}O)$_2$]$^{2+}$, that is, there is no incorporation of ^{18}O into the dioxoruthenium(VI) product. Analysis of the mass spectrum (−ve mode) of the permanganate remaining in the solution after 1 h indicates that it is ca. 60% ^{18}O-labeled. Independent experiments using [Ru^{VI}(tmc)(^{16}O)$_2$]$^{2+}$ in $H_2{}^{18}O$ at pH = 3 reviewed that the ruthenium(VI) oxo species remained as 100% [Ru^{VI}(tmc)(^{16}O)$_2$]$^{2+}$ after 2 h, indicating that there is no oxygen exchange with water during this period. For [Ru^{IV}(tmc)(O)(OH_2)]$^{2+}$ in $H_2{}^{18}O$ at pH = 3, the mass spectrum indicates a small amount of [Ru^{IV}(tmc)(^{18}O)]$^{2+}$ (5 ± 2%) after 2 h, indicating a slight exchange of the oxo ligand with water.

The ESI/MS for the reaction of [Ru^{IV}(tmc)(^{16}O)($NCCH_3$)](PF_6)$_2$ with K[$Mn^{16}O_4$] in $H_2{}^{18}O$ (97 atom % ^{18}O, pH = 3) was also investigated (Figure 8). In this case a peak at m/z = 196.4 gradually increases, and analysis of the isotopic pattern of this peak after 1.5 h indicates that it mainly consists of (90 ± 5)% [Ru^{VI}(tmc)(^{16}O)(^{18}O)]$^{2+}$ and (10 ± 5)% [Ru^{VI}(tmc)(^{16}O)$_2$]$^{2+}$. There is also a small amount of $K_2MnO_4^+$ at m/z = 197.4, which is also present in the MS of K[MnO_4] alone in water. MS/MS of this peak gives a fragment peak at m/z = 39 which is due to

(18) For all reactions in water, an equal volume of CH_3CN was added to the sample solution before electrospraying to increase the sensitivity of the MS signals. In the absence of CH_3CN the signals are extremely weak.

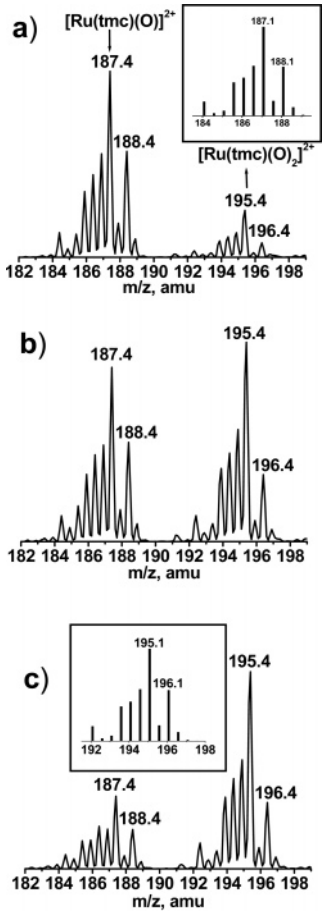

Figure 7. ESI/MS (+ve mode) of $[Ru^{IV}(tmc)(O)(NCCH_3)](PF_6)_2$ (0.3 mM) and $K[Mn^{18}O_4]$ (1.9 mM) in 1 mM CF_3COOH in H_2O at 296 K at different time intervals: (a) 5 min, (b) 30 min, (c) 60 min. The insets in panels a and c show the calculated isotopic patterns for $[Ru(tmc)(O)]^{2+}$ and $[Ru(tmc)(O)_2]^{2+}$, respectively.

K^+. These results again show that in the conversion of monooxoruthenium(IV) to dioxoruthenium(VI); the oxygen atom comes from water and not from permanganate.

3.3.2. Reaction in CH_3CN. The ESI/MS (+ve mode) of $[Ru^{IV}(tmc)(O)(NCCH_3)](PF_6)_2$ in CH_3CN shows a peak at *m*/*z* 187.4 which is due to $[Ru(tmc)(O)]^{2+}$ (Figure 9). Upon adding excess $K[Mn^{18}O_4]$ (90% ^{18}O-labeled), the peak at *m*/*z* 187.4 decreases with concomitant increase of a new peak at *m*/*z* 196.4. Analysis of the isotopic pattern of the *m*/*z* 196.4 peak after 24 h indicates that it is a mixture of (80 ± 5)% $[Ru(tmc)(^{16}O)(^{18}O)]^{2+}$ and (20 ± 5)% $[Ru(tmc)(^{16}O)_2]^{2+}$. Analysis of the MS of permanganate (−ve mode) indicates that exchange has occurred, the ^{18}O% decreases from the initial 90% to 77% after 7 h, and to 64% after 24 h. By taking into account this ^{18}O exchange, our results indicate that there is almost quantitative incorporation of oxygen atoms from potassium permanganate to the dioxoruthenium(VI) species.

3.4. Mechanism. 3.4.1. Reaction in Water. The mechanism for the oxidation of *trans*-$[Ru^{IV}(tmc)(O)(OH_2)]^{2+}$ to *trans*-$[Ru^{VI}(tmc)(O)_2]^{2+}$ by MnO_4^- in water may involve one of the following initial, rate-limiting steps:

(1) Electron transfer

$$[Ru^{IV}(tmc)(O)(OH_2)]^{2+} + [Mn^{VII}O_4]^- \rightarrow [Ru^{V}(tmc)(O)(OH_2)]^{3+} + [Mn^{VI}O_4]^{2-} \quad (12)$$

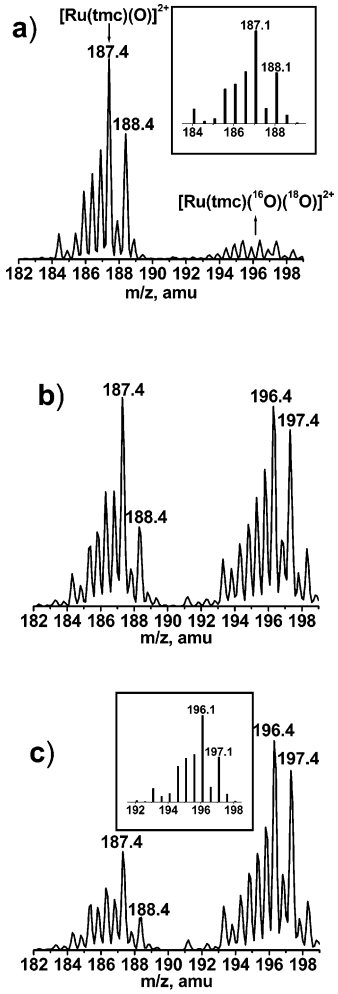

Figure 8. ESI/MS (+ve mode) of $[Ru^{IV}(tmc)(O)(NCCH_3)](PF_6)_2$ (0.3 mM) and $K[MnO_4]$ (1.9 mM) in $H_2{}^{18}O$ (pH = 3) at different time intervals: (a) 5 min, (b) 45 min, (c) 90 min. The inset in panel c shows the calculated isotopic pattern for 90% ^{18}O-labeled $[Ru(tmc)(^{16}O)(^{18}O)]^{2+}$ and 10% $[Ru(tmc)(^{16}O)_2]^{2+}$.

(2) Hydrogen-atom transfer

$$[Ru^{IV}(tmc)(O)(OH_2)]^{2+} + [Mn^{VII}O_4]^- \rightarrow [Ru^{V}(tmc)(O)(OH)]^{2+} + [Mn^{VI}O_3(OH)]^- \quad (13)$$

(3) Hydride transfer

$$[Ru^{IV}(tmc)(O)(OH_2)]^{2+} + [Mn^{VII}O_4]^- \rightarrow [Ru^{VI}(tmc)(O)(OH)]^{3+} + [Mn^{V}O_3(OH)]^{2-} \quad (14)$$

(4) Oxygen-atom transfer

$$[Ru^{IV}(tmc)(O)(OH_2)]^{2+} + [Mn^{VII}O_4]^- \rightarrow [Ru^{VI}(tmc)(O)_2]^{2+} + [Mn^{V}O_3]^- \quad (15)$$

In eq 15, the reduced manganese species is probably in the form of $[MnO_3(OH)]^{2-}$ or $[MnO_3(CH_3CN)_x]^-$, arising from combination of $[Mn^{V}O_3]^-$ with water or acetonitrile in the solvent cage.

E^0 for the MnO_4^-/MnO_4^{2-} couple is +0.56 V versus NHE.[12] E^0 for the $[Ru^{V/IV}(tmc)(O)(OH_2)]^{3+/2+}$ couple is not known, but should be much higher than the E^0 for the $[Ru^{V/IV}(tmc)(O)(Cl)]^{2+/+}$ couple, which is ca. 1.05 V versus $Cp_2Fe^{+/0}$ in CH_3-

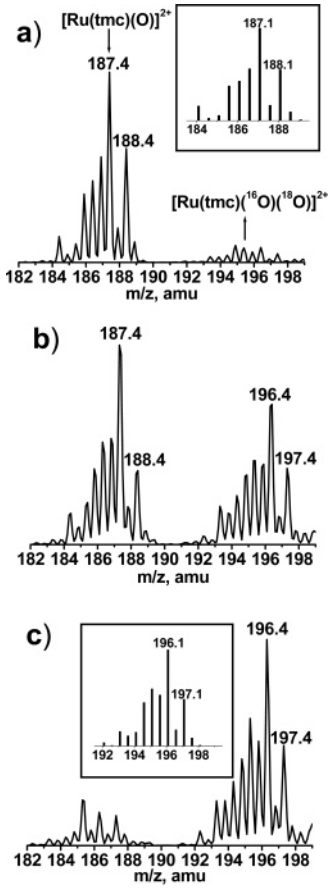

Figure 9. The ESI/MS (+ve mode) of $[Ru^{IV}(tmc)(O)(NCCH_3)](PF_6)_2$ (3 mM) and $K[Mn^{18}O_4]$ (25 mM) in CH_3CN at different time intervals: (a) 1 h, (b) 7 h, (c) 24 h. The insets in panels a and c show the calculated isotopic patterns for $[Ru(tmc)(O)]^{2+}$ and 80% $[Ru(tmc)(^{16}O)(^{18}O)]^{2+}$ + 20% $[Ru(tmc)(^{16}O)_2]^{2+}$, respectively.

CN (ca. 1.67 V versus NHE),[19] since the anionic Cl^- should stabilize high oxidation states better than the neutral H_2O. Thus the electron-transfer step is expected to be uphill by over 1.0 V, which is highly unfavorable.

On the other hand the large deuterium and oxygen isotope effects of 3.9 and 1.3, respectively, suggest that the rate-limiting step involves O−H cleavage. This is consistent with either a hydrogen-atom transfer (eq 13) or hydride transfer (eq 14) mechanism, which cannot be easily distinguished for this system. Hydrogen-atom transfer would result in the formation of *trans*-$[Ru^V(tmc)(O)(OH)]^{2+}$, however this species would not be observed because it is known to disproportionate rapidly in acidic medium to give *trans*-$[Ru^{VI}(tmc)(O)_2]^{2+}$ and *trans*-$[Ru^{IV}(tmc)(O)(OH_2)]^{2+}$.[6b] On the other hand, hydride transfer would produce *trans*-$[Ru^{VI}(tmc)(O)(OH)]^{3+}$ initially, which would then undergo rapid deprotonation to give *trans*-$[Ru^{VI}(tmc)(O)_2]^{2+}$. The free energy change (ΔG^0) for the hydrogen-atom transfer step can be evaluated according to Scheme 2.

Bond dissociation energies (BDEs) are usually used in discussions of hydrogen-atom transfer reactions.[4,17,20−21] Since the entropy change (ΔS^0) for the hydrogen-atom transfer step is usually close to zero,[4,17,20−21] $\Delta G^0 \approx \Delta H^0$; ΔH^0 is the difference between O−H BDE of $[O{=}Ru^{IV}(tmc)(HO-H)]^{2+}$ and $[Mn^{VI}(O)_3(O-H)]^-$. The BDE of $[O{=}Ru^{IV}(tmc)(HO-H)]^{2+}$ in water is calculated to be 81.9 kcal mol^{-1} by using the equation $BDE[O{=}Ru^{IV}(tmc)(OH-H)] = 23.06E^0 + 1.37pK_a + C$,[20−25] $C = 57$ kcal mol^{-1}.[17] The BDE of $[Mn^{VI}(O)_3(O-H)]^-$ has been evaluated to be 80 kcal mol^{-1}.[17]

Although the free energy for hydride-transfer can also be obtained by using a similar thermochemical cycle,[20−26] it was not evaluated since E^0 for $[Mn^{VI/V}(O)_3(OH)]^{1-/2-}$ and $[Ru^{VI/V}(tmc)(O)(OH)]^{3+/2+}$ are not known. However since hydride abstraction by MnO_4^- would produce $HMnO_4^{2-}$ which is a highly unstable species in acidic solution ($E^0 = 2.95$ V at pH = 0),[27] the hydride transfer pathway should be much more uphill than the hydrogen-atom transfer pathway. Moreover hydride transfer should be intrinsically slower than hydrogen-atom transfer because of larger solvent reorganization energy for transfer of a charged species.[26] Hence we conclude that the oxidation of *trans*-$[Ru^{IV}(tmc)(O)(OH_2)]^{2+}$ by MnO_4^- in aqueous solutions most likely occurs by an initial hydrogen-atom transfer mechanism. Although a relatively strong O−H bond has to be broken (81.9 Kcal mol^{-1}), an almost equally strong bond is formed (80 Kcal mol^{-1}) in the hydrogen-atom transfer step; hence $\Delta G^{\ddagger}$ is relatively small (15.6 kcal mol^{-1}). Mayer has shown that $\Delta G^{\ddagger}$ is related to ΔG^0 by the Marcus cross-relation for a number of hydrogen-atom transfer reactions.[28]

The rate constant for the oxidation of Ru^{IV} by $HMnO_4$ is faster than that by MnO_4^- by a factor of 3.8×10^3. Since the pathway for the oxidation of Ru^{IV} by $HMnO_4$ also exhibits a large deuterium isotope effect (4.9), it probably also occurs by initial hydrogen-atom transfer. ΔG^0 for this hydrogen-atom transfer process was not evaluated because the pK_a of H_2MnO_4 is unknown. However, since it has a much larger E^0 of 1.11 V,[29] it should be a much better hydrogen-atom abstracting agent than MnO_4^-.

Similar intermetal hydrogen-atom transfer (or proton-coupled electron transfer) mechanisms have been proposed for the comproportionation of polypyridyl complexes of oxoruthenium(IV) and aquaruthenium(II).[30] The disproportionation of aquachromium(IV) is also proposed to occur by hydrogen-atom transfer.[31]

3.4.2. Reaction in Acetonitrile. In acetonitrile *trans*-$[Ru^{IV}(tmc)(O)(NCCH_3)]^{2+}$ is quantitatively oxidized to *trans*-$[Ru^{VI}(tmc)(O)_2]^{2+}$ by MnO_4^-. Using $K[Mn(^{18}O)_4]$ the predominant ruthenium product is *trans*-$[Ru^{VI}(tmc)(^{16}O)(^{18}O)]^{2+}$, which is consistent with an oxygen-atom transfer mechanism shown in eq 15. The resulting MnO_3^- species presumably then undergoes rapid disproportionation to give MnO_4^- and MnO_2.

Some exchange of $K[Mn(^{18}O)_4]$ with $H_2{}^{16}O$ in CH_3CN was found to occur during the reaction with $[Ru^{IV}(tmc)(O)(N-$

(19) Wong, K. Y.; Che, C. M.; Anson, F. C. *Inorg. Chem.* **1987**, *26*, 737−741.
(20) Mayer, J. M. *Acc. Chem. Res.* **1998**, *31*, 441−450.
(21) Mayer, J. M. *Biomimetic Oxidations Catalyzed by Transition Metal Complexes*; Meunier, B., Ed.; Imperial College Press: London, 2000; pp 1−43.
(22) Wayner, D. D. M.; Lusztyk, E.; Pagé, D.; Ingold, K. U.; Mulder, P.; Laarhoven, L. J. J.; Aldrich, H. S. *J. Am. Chem. Soc.* **1995**, *117*, 8737−8744.
(23) Bordwell, F. G.; Liu, W. Z. *J. Am. Chem. Soc.* **1996**, *118*, 8777−8781.
(24) Parker, V. D. *J. Am. Chem. Soc.* **1992**, *114*, 7458−7462.
(25) Tilset, M.; Parker, V. D. *J. Am. Chem. Soc.* **1989**, *111*, 6711−6717.
(26) Matsuo, T.; Mayer, J. M. *Inorg. Chem.* **2005**, *44*, 2150−2158.
(27) Hlooeman, A. F.; Wiberg, E. *Inorg. Chem.*, Academic Press: San Diego, CA. 2001.
(28) Roth, J. P.; Yoder, J. C.; Won, T.-J.; Mayer, J. M. *Science* **2001**, *294*, 2524−2526.
(29) McAllister, R.; Hicks, K. W.; Hurless, M. A.; Pittenger, S. T.; Gedridge, R. W. *Inorg. Chem.* **1982**, *21*, 4098−4100.
(30) (a) Farrer, B. T.; Thorp, H. H. *Inorg. Chem.* **1999**, *38*, 2497−2502. (b) Binstead, R. A.; Meyer, T. J. *J. Am. Chem. Soc.* **1987**, *109*, 3287−3297.
(31) Nemes, A.; Bakac, A. *Inorg. Chem.* **2001**, *40*, 2720−2724.

Scheme 2

$$[Mn^{VII}O_4]^- + e^- \longrightarrow [Mn^{VI}O_4]^{2-} \qquad E^0 = 0.564\ V\ ^{12},\ \Delta G = -13.0\ kcal\ mol^{-1}$$

$$[Mn^{VI}O_4]^{2-} + H^+ \longrightarrow [Mn^{VI}(O)_3(OH)]^- \qquad pK_a = 7.4\ ^{17},\ \Delta G = -10.1\ kcal\ mol^{-1}$$

$$[Ru^{IV}(tmc)(O)(OH_2)]^{2+} \longrightarrow [Ru^{IV}(tmc)(O)(OH)]^+ + H^+ \qquad pK_a = 4.7,\ \Delta G = 6.4\ kcal\ mol^{-1}$$

$$[Ru^{IV}(tmc)(O)(OH)]^+ \longrightarrow [Ru^{V}(tmc)(O)(OH)]^{2+} + e^- \qquad E^0 = 0.80\ V,\ \Delta G = 18.5\ kcal\ mol^{-1}$$

$$[Mn^{VII}O_4]^- + [Ru^{IV}(tmc)(O)(OH_2)]^{2+} \longrightarrow [Mn^{VI}(O)_3(OH)] + [Ru^{V}(tmc)(O)(OH)]^{2+} \qquad \Delta G^0 = 1.8\ kcal\ mol^{-1}$$

$CCH_3)]^{2+}$, although potassium permanganate alone does not exchange with water for at least 24 h at room temperature. One possible explanation is the oxygen exchange is catalyzed by $[MnO_3]^-$ according to

$$[Ru^{IV}(tmc)(^{16}O)(OH_2)]^{2+} + [Mn^{VII}(^{18}O)_4]^- \rightleftharpoons [Ru^{VI}(tmc)(^{18}O)(^{16}O)]^{2+} + [Mn^{V}(^{18}O)_3]^- \quad (16)$$

$$[Mn^{V}(^{18}O)_3]^- + H_2{}^{16}O \rightleftharpoons [Mn^{V}(^{18}O)_2(^{16}O)]^- + H_2{}^{18}O \quad (17)$$

$$[Mn^{V}(^{18}O)_2(^{16}O)]^- + [Mn^{VII}(^{18}O)_4]^- \rightleftharpoons [Mn^{VII}(^{18}O)_3(^{16}O)]^- + [Mn^{V}(^{18}O)_3]^- \quad (18)$$

$[MnO_3]^-$ should not catalyze the exchange of $[Ru^{VI}(tmc)(O)_2]^{2+}$ with water, otherwise the observed amount of $[Ru^{VI}(tmc)(^{16}O)(^{18}O)]^{2+}$ should be less than 80%.

The reaction in CH_3CN is about ten times slower than in water, which is due to a slightly higher $\Delta H^{\ddagger}$ in CH_3CN, while $\Delta S^{\ddagger}$ is similar for the two solvents. In water, the oxygen-atom transfer pathway may be even slower since water is likely to be a better donor ligand than acetonitrile. Intermetal oxygen-atom transfer has been demonstrated for various metal porphyrin complexes.[3,32] Oxygen-atom transfer in various nonheme $Fe^{IV}{=}O/Fe^{II}$,[33] $Ir^{V}{=}O/Ir^{III}$ and $Os^{V}{=}O/Os^{III}$ systems[34] have also been reported.

Conclusion

Hydrogen-atom transfer and oxygen-atom transfer are fundamental processes in chemical and biological systems. The oxidation of *trans*-$[Ru^{IV}(tmc)(O)(solv)]^{2+}$ by MnO_4^- in both water and acetonitrile results in the formation of *trans*-$[Ru^{VI}(tmc)(O)_2]^{2+}$. Although the reactions in the two solvents have similar rates and activation parameters, in water the reaction occurs by initial rate-limiting hydrogen-atom transfer, while that in acetonitrile occurs by oxygen-atom transfer. Large deuterium as well as oxygen isotope effects are observed for reactions in water.

Acknowledgment. The work described in this paper was supported by the Research Grants Council of Hong Kong (CityU 101403) and the City University of Hong Kong (Grant 7001582).

Supporting Information Available: Table and figures of rate data, UV−vis spectrum. This material is available free of charge via the Internet at http://pubs.acs.org.

JA074282F

(32) (a) Hays, J. A.; Day, C. L.; Young, V. G., Jr.; Woo, L. K. *Inorg. Chem.* **1996**, *35*, 7601−7607. (b) Woo, L. K.; Hays, J. A.; Goll, J. G. *Inorg. Chem.* **1990**, *29*, 3916−3917. (c) Balch, A. L.; Chan, Y.-W.; Cheng, R.-J.; La Mar, G. N.; Latos-Grazynski, L.; Renner, M. W. *J. Am. Chem. Soc.* **1984**, *106*, 7779−7785. (d) Chin, D.-H.; La Mar, G. N.; Balch, A. L. *J. Am. Chem. Soc.* **1980**, *102*, 5945−5947.

(33) Sastri, C. V.; Oh, K.; Lee, Y. J.; Seo, M. S.; Shin, W.; Nam, W. *Angew. Chem., Int. Ed.* **2006**, *45*, 3992−3995.

(34) Fortner, K. C.; Laitar, D. S.; Muldoon, J.; Pu, L.; Braun-Sand, S. B.; Wiest, O.; Brown, S. N. *J. Am. Chem. Soc.* **2007**, *129*, 588−600.